Article

Journal of Intelligent Material Systems and Structures

Journal of Intelligent Material Systems and Structures
23(1) 25–33

DOI: 10.1177/1045389X11429853
jim.sagepub.com
SAGE

Development of a real-time tunable stiffness and damping vibration isolator based on magnetorheological elastomer

G. J. Liao, X-L Gong, S. H. Xuan, C. J. Kang and L. H. Zong

Abstract

A tunable stiffness and damping vibration isolator based on magnetorheological elastomers (MREs) is developed. In this isolator, four MRE elements are used as the tunable springs, whose stiffness can be controlled by varying the magnetic field. A voice coil motor, which is controlled by the relative velocity feedback of the payload, is used as the tunable damper of the isolator. Under the combined ON–OFF control, the proposed vibration isolator shows satisfying isolation effect. The experimental results indicate that the responses of the payload are suppressed significantly in comparison to the passive system. The transmissibility of the payload around the resonant frequency is decreased by 61.5%. The root mean square (RMS) value and the maximum value of the displacement responses of the payload are decreased by 36.0% and 50.0%, respectively. In addition, the RMS values and maximum values of the velocity responses are decreased by 45.4% and 52.5%, respectively.

Keywords

ON–OFF control, MRE, voice coil motor, isolator, variable stiffness and damping

Introduction

Recently, vibration isolation systems have been intensively studied and widely used in applications. The vibration isolation control systems can be divided into passive, active, and semiactive (SA). The SA vibration isolation systems are the compromise of passive systems and active systems, and they only expend quite a small amount of energy to vary their parameters to improve the performance, such as damping and/or stiffness. One common SA vibration isolation system is the tunable damping system, which has been proven to be an effective vibration control technique (Dyke et al., 1998; Yu et al., 2009; Zhou et al., 2008). These tunable damping systems consisting of passive springs and tunable dampers show high performance, and some of them can even approach an ideal fully active system. Besides, tuning the stiffness of the vibration isolation system is another method in a SA system. A few researchers have proposed some vibration isolation systems with tunable stiffness to prove their effectiveness (Liu et al., 2008; Nagarajaiah and Sonmez, 2007; Yang et al., 1996).Yang et al. (1996) proposed a controllable stiffness system to suppress buildings' response to earthquakes. Nagarajaiah and Sonmez (2007) developed a class of single or multiple SA variable stiffness-tuned mass dampers, which can be used for response control of multistory structures. Recently, Liu et al. (2008) proposed a SA vibration isolation system with variable stiffness and damping using magnetorheological fluid (MRF) dampers. However, the tunable stiffness vibration isolation system has not been thoroughly investigated due to the complexity and high cost. Therefore, a new tunable stiffness vibration isolation system with simple structure and low cost needs to be developed.

Magnetorheological elastomers (MREs) are a kind of function materials whose shear modulus can be controlled rapidly, continuously, and reversibly by applying an external magnetic field (Ginder et al., 1999; Li and Zhang, 2010; Xu et al., 2010). They comprise

CAS Key Laboratory of Mechanical Behavior and Design of Materials, Department of Modern Mechanics, University of Science and Technology of China, Hefei, China

Corresponding author:
Xing-long Gong, CAS Key Laboratory of Mechanical Behavior and Design of Materials, Department of Modern Mechanics, University of Science and Technology of China, Hefei 230027, China
Email: gongxl@ustc.edu.cn

microsized magnetic particles dispersed in elastomers or rubberlike materials. The magnetic particles form chainlike or columnar structures, which are fixed in the polymer matrix after curing. Due to their special structure, MREs overcome the problems of deposition, environmental contamination, and sealing existing in MRFs (Carlson and Jolly, 2000; Chen et al., 2008; Farshad and Le Roux, 2005; Popp et al., 2010) and attract considerable attention in recent years (Deng et al., 2006; Ginder et al., 1999, 2001; Gong et al., 2005; Lerner and Cunefare, 2008; Ni et al., 2009). Many studies reported the applications of MREs to adaptive tuned vibration absorbers. Ginder et al. (2001) did the pioneer study on the development of an adaptive tunable vibration absorber using MREs. Deng et al. (2006) used MREs to design a tunable vibration absorber with a frequency range of 55–82 Hz. Lerner and Cunefare (2008) developed three vibration absorber configurations with MREs in shear, longitudinal, and squeeze modes, respectively. Ni et al. (2009) proposed a dynamic stiffness-tuning absorber with squeeze-strain–enhanced MREs.

Besides vibration absorbers, MREs can also be used in vibration isolator due to their excellent stiffness tunable nature. Ginder et al. (2000) used MREs to construct a proof-of-concept mounting and isolation in automotive. Hitchcock et al. (2006) proposed a device based on MREs to control the response of a structure to shock events. Opie and Yim (2009) investigated a tunable stiffness MRE vibration isolator, and the experimental results showed that MRE isolator with SA controller system reduced resonances and payload velocities by 16%–30% when compared to passive systems. Due to their high efficiency and facility, the development of MRE-based isolator has become a pressing need. In addition, real-time tunable vibration isolators are more advantageous than the passive isolator, such as metal rubber isolator, because the resonance can be significantly decreased, while the good high-frequency isolation effect is still maintained.

In this study, a novel MRE-based vibration isolator with tunable stiffness and damping is proposed. MREs are used as the tunable spring elements, and a customized voice coil motor controlled by the relative velocity feedback is used as a variable damper. Compared to the conventional device with variable stiffness, the proposed vibration isolator is very simple and easy to be applied in practical system. The article is divided into six sections. Following the introduction, the method of MRE fabrication and its mechanical characteristics are introduced. The control strategies of the isolator are analyzed in 'Control Strategies' section. 'Structure of the MRE-Based Vibration Isolator' section describes the structure of the MRE-based vibration isolator. 'Experiments and Simulations' section shows the experimental and simulation results, and the conclusions are summarized in 'Conclusion' section.

MRE Fabrication and Its Characteristics

MRE Fabrication

The materials of fabricated MRE samples consist of carbonyl iron particles (Type CN, with the average diameter of 6 μm; BASF Company, Germany), high-temperature vulcanization (HTV) silicone rubber (Type MVQ 110-2; Dong Jue Fine Chemicals Nanjing Co., Ltd. Nanjing, China)., methyl silicone oil (Shanghai Resin Factory Co., Ltd. Shanghai, China), and vulcanizing agent (double methyl double benzoyl hexane; Shenzhen Gujia Company, Shenzhen, China). The methyl silicone oil, viscosity of 50 cP, was used as plasticizer to improve the processing of rubber mixing.

First, the HTV silicone rubber was subjected to heat treatment at 150°C for 4 h to reduce the air in the rubber. Then, the rubber was placed in a double-roll mill (Model XK-160; Taihu rubber Machinery Inc., China) to be thoroughly mixed with iron particles, silicone oil, and vulcanizing agent for about 1 h. Later, the rubber mixture was used to fabricate MRE samples. During the fabrication, a prestructure method was used, which can significantly enhance the magnetorheological effect of MRE. The rubber mixture was placed into a mold. Then, the mold was fixed to a customized magnet-heat-coupled device, as shown in Figure 1. This device can keep the rubber mixture at a fixed temperature and can supply a vertical magnetic field. The temperature in the prestructure process was 120°C, and the magnetic field was about 1.5 T. The prestructure process lasted for 15 min. Then, the mold with the rubber mixture was placed on a flat vulcanizer (Model BL-6170-B; Bolon Precision Testing Machines Co., China) for vulcanizing. The vulcanizing process was carried out at a temperature of 160°C for 5 min. After that, the MRE samples were obtained.

Mechanical Characteristics

The dynamic shear modulus of the as-prepared MRE under various magnetic flux densities was tested using a modified dynamic mechanical analyzer (Model Tritec 2000; Triton technology Co., Ltd., UK). Figure 2 shows

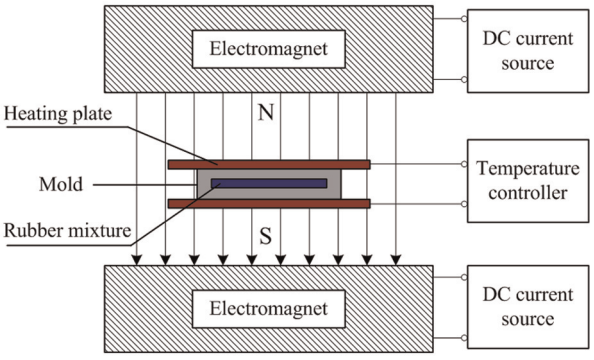

Figure 1. Sketch of a customized magnet-heat-coupled device.

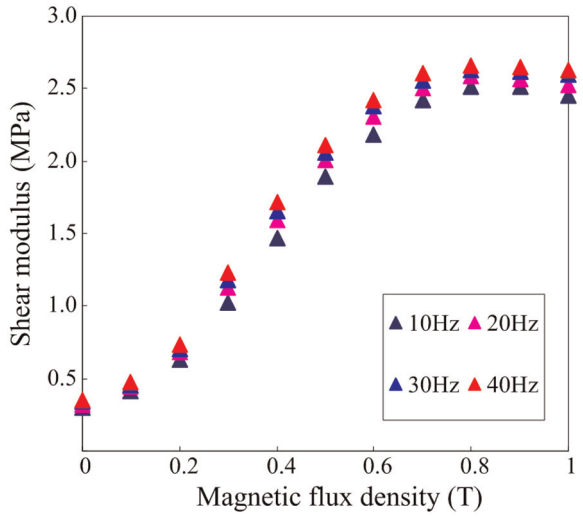

Figure 2. Dynamic shear modulus of MRE under various magnetic flux densities.

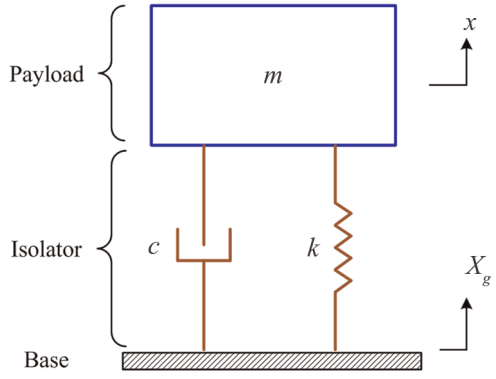

Figure 3. A single-degree-of-freedom system.

the relationship between the shear modulus of MRE and the magnetic flux density under different testing frequencies. From the figure, it can be seen that the initial shear modulus of MRE is around 0.3 MPa, and saturation shear modulus is around 2.5 MPa. The relative shear modulus change is as high as about 700%. Such unique high MR effect makes the fabricated MREs to be a good candidate for the stiffness element of vibration isolator.

Control Strategies

Sinusoid Excitation

The mathematical model of a vibration isolation system can be represented by a single-degree-of-freedom system (Figure 3). As shown in Figure 3, m is the mass of the payload; c and k are the damping coefficient and the stiffness of the isolator, respectively; x and x_g are the displacements of the payload and the ground base,

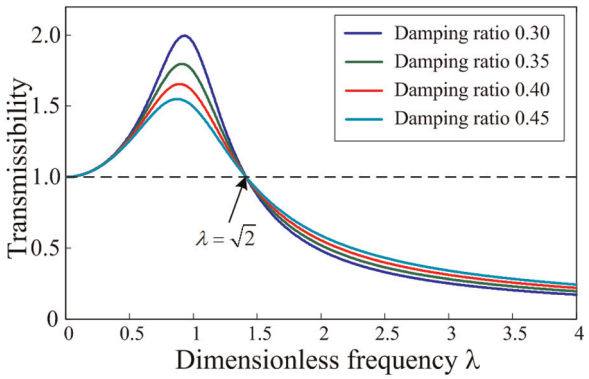

Figure 4. Transmissibility of a single-degree-of-freedom system.

respectively. The equation of motion for the system is as follows:

$$m\ddot{x} + c\dot{x} + kx = c\dot{x}_g + kx_g \tag{1}$$

where $(\ddot{\cdot})$ and $(\dot{\cdot})$ mean $\mathrm{d}^2/\mathrm{d}t^2$ and $\mathrm{d}/\mathrm{d}t$. The transmissibility of the system is

$$T = \frac{X}{X_g} = \sqrt{\frac{1 + (2\xi\lambda)^2}{(1-\lambda^2)^2 + (2\xi\lambda)^2}} \tag{2}$$

where

$$\lambda = \frac{\omega}{\omega_0}, \quad \omega_0 = \sqrt{\frac{k}{m}}, \quad \xi = \frac{c}{2\sqrt{km}}$$

and ω is the excitation frequency; ω_0 is the nature frequency of the isolation system; X and X_g are the amplitudes of x and x_g, respectively. Figure 4 shows the relationship between the transmissibility and the dimensionless frequency λ.

From Figure 4, it can be seen that when $\lambda < \sqrt{2}$, the vibration of the payload is severer than the excitation base; when $\lambda > \sqrt{2}$, the vibration of the payload is weaker than the base. In other words, when the excitation frequency ω is smaller than $\sqrt{2}\omega_0$, there is no isolation effect for the vibration isolation system. If $\lambda < \sqrt{2}$, the vibration of the payload decreases with increasing of the damping (Figure 4). Meanwhile, the vibration of the payload increases with increasing of the damping when $\lambda > \sqrt{2}$. According to the features of the transmissibility of a single-degree-of-freedom system, the control law can be summarized as follows. When the excitation frequency ω is larger than $\sqrt{2}\omega_0$, smaller stiffness and damping are of benefit to decreasing the vibration of the payload. When the excitation frequency ω is around the nature frequency of the system, the increasing of the stiffness will shift the nature frequency away from the excitation frequency, and the increasing of the damping will lead to the decreasing of the vibration. Thus, the vibration of the payload is

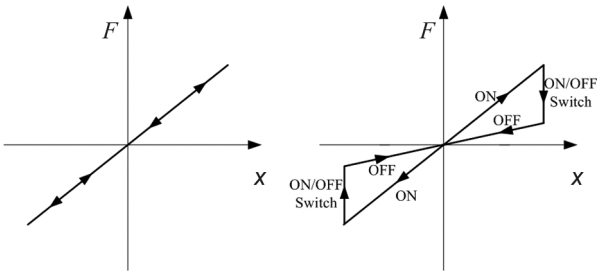

Figure 5. Stiffness ON–OFF control.

attenuated. Therefore, the control laws of MRE-based vibration isolator under sinusoid excitation can be expressed as

$$\begin{cases} k = k_{\max} \text{ and } c = c_{\max} & \text{if } \omega \leqslant \sqrt{2}\omega_0 \\ k = k_{\min} \text{ and } c = c_{\min} & \text{if } \omega > \sqrt{2}\omega_0 \end{cases} \tag{3}$$

where $k_{\max}$ and $k_{\min}$ are the maximum and minimum stiffness of MRE-based vibration isolator, respectively. The $c_{\max}$ and $c_{\min}$ are the maximum and minimum damping of MRE-based vibration isolator, respectively.

Random Excitation

Beside the sinusoid excitation, another kind of excitation is random excitation, which is quite common in road excitation, seismic excitation, and so on. Therefore, it is necessary to investigate the control laws for MRE-based vibration isolator under random excitation. For damping force control, the ON–OFF control laws can be expressed as (Jansen and Dyke, 2000; Liu et al., 2005)

$$c = \begin{cases} c_{\max} & \text{if } x_r \dot{x}_r \geq 0 \\ c_{\min} & \text{if } x_r \dot{x}_r < 0 \end{cases} \tag{4}$$

where x_r and $\dot{x}_r$ are the payload's displacement and velocity with respect to the base, respectively. $x_r \dot{x}_r \geq 0$ means the payload is moving away from the balance position.

For stiffness control, the ON–OFF control has attracted considerable attention in recent years (Nagarajaiah and Sonmez, 2007; Yang et al., 1996, 2000). The basic principle is shown in Figure 5, where F is the elastic force generated by the spring and x is the deformation of the spring. It can be seen from Figure 5 that the elastic force dose not dissipate energy without ON–OFF control. However, under proper ON–OFF control laws, the elastic force dissipates energy so as to weaken the vibration of the payload. Similar to the damping force ON–OFF control laws, the stiffness ON–OFF control laws can be expressed as (Yang et al., 1996, 2000):

$$k = \begin{cases} k_{\max} & \text{if } x_r \dot{x}_r \geq 0 \\ k_{\min} & \text{if } x_r \dot{x}_r < 0 \end{cases} \tag{5}$$

where x_r and $\dot{x}_r$ have the same meaning with the damping force ON–OFF control laws. Combining stiffness control and damping control, the control laws for MRE-based vibration isolator can be expressed as

$$\begin{cases} k = k_{\max} \text{ and } c = c_{\max} & \text{if } x_r \dot{x}_r \geq 0 \\ k = k_{\min} \text{ and } c = c_{\min} & \text{if } x_r \dot{x}_r < 0 \end{cases} \tag{6}$$

Structure of the MRE-Based Vibration Isolator

The scheme of the proposed MRE-based vibration isolator is shown in Figure 6. It can be seen that MRE-based vibration isolator consists of eight parts: base, magnetic excitation coil, magnetic conductor, shear plate, iron core, MRE, voice coil motor, and mounting plate. Four MRE samples, working in shear mode, are used as the stiffness elements. In this system, they are designed to bear the payload. The base, iron core, magnetic conductor, and part of shear plate form two closed C-shaped magnetic circulates. The magnetic field is created by three coils, and it can be controlled by the coil current. The MRE samples were connected to the mounting plate by two shear plates. A voice coil motor is fixed between the magnetic conductor and the mounting plate. The stator of the voice coil motor is fixed on the magnetic conductor, and the mover is connected to the mounting plate.

The voice coil motor is controlled by the relative velocity feedback of the payload with respect to the base. The force generated by the voice coil motor can be expressed as

$$f_{act} = -g\dot{x}_r \tag{7}$$

where g is the feedback gain and $\dot{x}_r$ is the relative velocity of the payload with respect to the base. In comparison to the damping force, the force generated by the voice coil motor is similar to the damping force for both kinds of force are proportional to the relative velocity. Therefore, under the relative velocity feedback control,

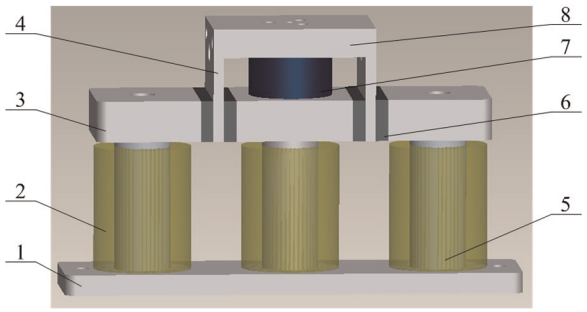

Figure 6. Sketch of the MRE-based vibration isolator: 1, base; 2, magnetic excitation coil; 3, magnetic conductor; 4 shear plate; 5, iron core; 6, MRE; 7, voice coil motor; 8, mounting plate.

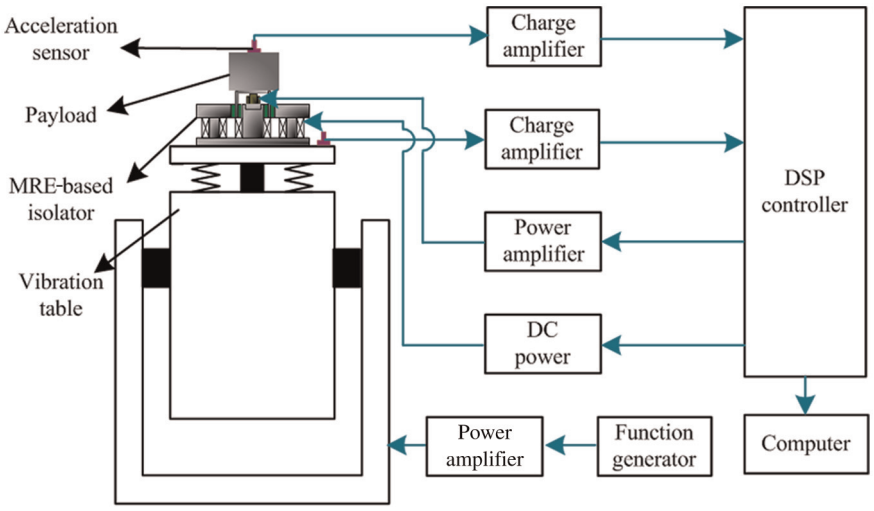

Figure 7. Experimental setup for the MRE-based vibration isolator.

the voice coil motor can be used as a damper, whose damping coefficient is equal to the feedback gain g.

The two most important parts of the MRE-based vibration isolator are MRE and the voice coil motor. Though the relationship between the applied current I and the stiffness k is nonlinear and cannot be accurately expressed, maximal I leads to maximal k and minimal I leads to minimal K. By applying a maximum current $I_{\max}$ or a minimum current $I_{\min}$, the stiffness of the isolator can be varied between $k_{\max}$ and $k_{\min}$. By turning on or turning off the voice coil motor, the damping of the isolator can be varied between $c_{\max}$ and $c_{\min}$.

Finally, the control laws of MRE-based vibration isolator can be summarized as

$$\text{Sinusoid excitation}: \begin{cases} I = I_{\max} \text{ and } g = g_{\max} & \text{if } \omega \leqslant \sqrt{2}\omega_0 \\ I = I_{\min} \text{ and } g = g_{\min} & \text{if } \omega > \sqrt{2}\omega_0 \end{cases} \tag{8}$$

$$\text{Random excitation}: \begin{cases} I = I_{\max} \text{ and } g = g_{\max} & \text{if } x_r \dot{x}_r \geq 0 \\ I = I_{\min} \text{ and } g = g_{\min} & \text{if } x_r \dot{x}_r < 0 \end{cases} \tag{9}$$

where I is the current applied to the magnetic excitation coil and g is the relative velocity feedback gain.

Experiments and Simulations

Experimental Setup

Figure 7 shows the experimental setup for investigating the performance of MRE-based vibration isolator. The prototype was mounted on the vibration table (Model DY-300-2; Suzhou Sushi Testing Instrument Co., Ltd. Suzhou, China.). A mass block, used as payload, was fixed on the mounting plate of the isolator. Two accelerometers (Model CA-YD-107; Sinocera Piezotronics Inc., China) were used to measure the acceleration responses of the base and the payload. The acceleration signals were sent to a customized digital signal processor (DSP) controller as the input signals of the prototype. For sinusoid excitation, the excitation frequency was obtained using a fast Fourier transform (FFT) analysis. For random excitation, the relative velocity and displacement of the payload with respect to the base were obtained by integrating the acceleration signals. According to the control laws shown in Equations (8) and (9), the DSP controller calculated the control signals of the magnetic excitation coil and the voice coil motor. Then, the two control signals were sent to a power amplifier and a DC power source to drive the voice coil motor and the magnetic excitation coil. In this experiment, the computer was used to collect and store the concerned signals transported by the DSP controller.

Frequency Response to Sinusoid Base Excitations

The steady-state response to a sinusoid base excitation is shown in Figure 8, where the frequency is changed from 2.5 to 18.75 Hz. Generally, for a vibration isolation system, the isolation efficiency increases with

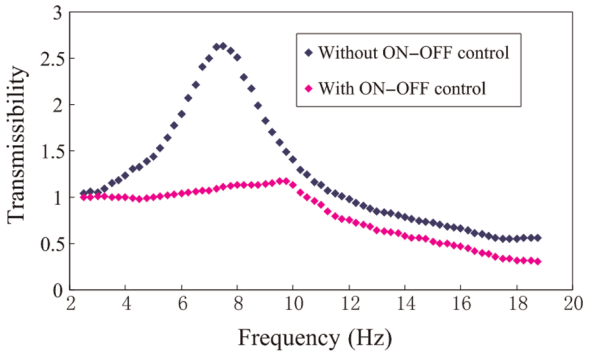

Figure 8. Frequency response to sinusoid base excitations.

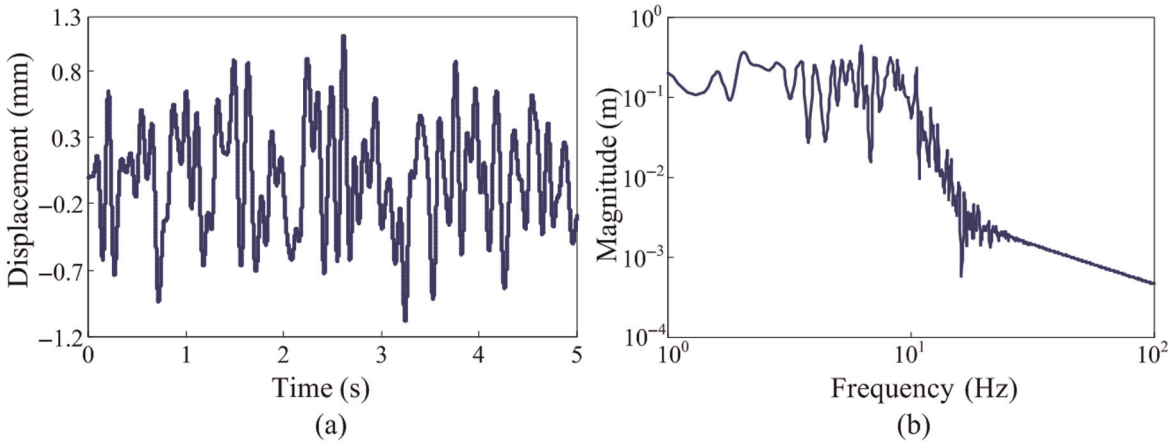

Figure 9. Random excitation: (a) time history and (b) frequency spectrum.

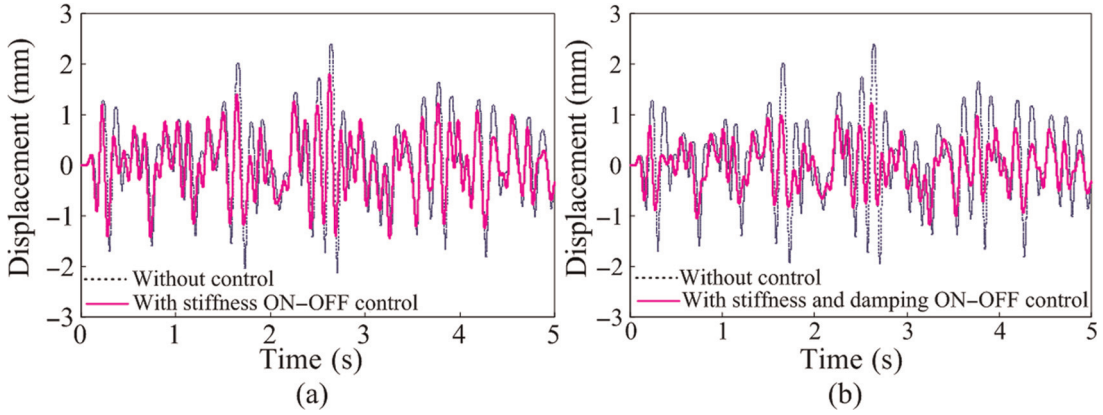

Figure 10. Displacement response of the payload: (a) stiffness ON–OFF control and (b) stiffness and damping ON–OFF control.

increasing of the excitation frequency. Due to this reason, the frequency range in the experiment was chosen from 2.5 to 18.75 Hz. From Figure 8, it can be seen that the nature frequency of the vibration isolation system is 7.5 Hz. Compared to the vibration without ON–OFF control, the vibration of the payload with ON–OFF control in the whole experimental frequency range is significantly suppressed. Surprisingly, the transmissibility decreases to about 1 from about 2.6, and the relative change is around 61.5% at the resonant frequency, which clearly indicates that the present vibration isolation system shows a well efficiency. In this experiment, $I_{max} = 1$ A, $I_{min} = 0$ A, $g_{max} = 1000$ Ns/m, and $g_{min} = 0$ Ns/m.

Response to Random Base Excitations

Figure 9(a) shows the time history of a random base excitation. Figure 9(b) shows its frequency spectrum. The random signals are the uniform distribution signals filtered by a band-pass filter. Since the vibration of the payload around nature frequency is the severest and the isolation efficiency increases with increasing of the frequency, the frequency range of the random excitation was chosen around the resonant frequency.

Figures 10 and 11 show the response of the payload under different control laws. Figures 10(a) and 11(a) show the response data that were obtained with and without the stiffness ON–OFF control. Here, stiffness ON–OFF control means only the stiffness is controlled, and the relative velocity feedback gain is fixed at zero during the experiment. Figures 10(b) and 11(b) compare the response without control to the response with stiffness and damping ON–OFF control. From the figures, it can be seen that the vibration of the payload was significantly suppressed under the control algorithm. In comparison to a single stiffness ON–OFF control, stiffness and damping double ON–OFF control performs better.

The RMS values and the maximum values of the response of the payload are tabulated in Table 1, where S ON–OFF control means stiffness ON–OFF control and S + D ON–OFF control means stiffness and

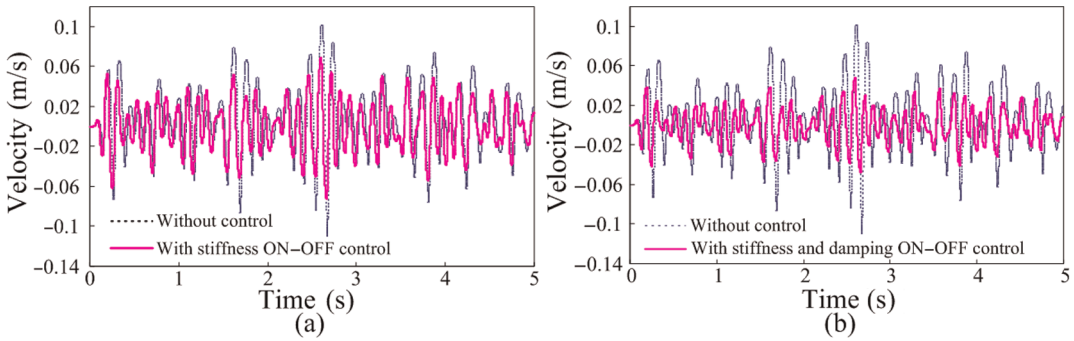

Figure 11. Velocity response of the payload: (a) stiffness ON–OFF control and (b) stiffness and damping ON–OFF control.

Table 1. RMS values and maximum values of the response to random excitations.

	RMS values		Maximum values	
	x (mm)	$\dot{x}$ (m/s)	x (mm)	$\dot{x}$ (m/s)
Without control	0.78	0.033	2.4	0.101
S ON–OFF control	0.60	0.026	1.8	0.068
S + D ON–OFF control	0.45	0.018	1.2	0.048

RMS: root mean square; S ON–OFF: stiffness ON–OFF control; S + D ON–OFF: stiffness + damping force ON–OFF control.

damping ON–OFF control. As shown in the table, the RMS values and maximum values of the payload's responses are significantly decreased by the control algorithm. Comparing the two control algorithms, S + D ON–OFF control performs better than S ON–OFF control. Under the S + D ON–OFF control, the RMS value and maximum value of the displacement responses of the payload are decreased by 36.0% and 50.0%, respectively. Meanwhile, the RMS value and maximum value of the velocity responses are decreased by 45.4% and 52.5%, respectively.

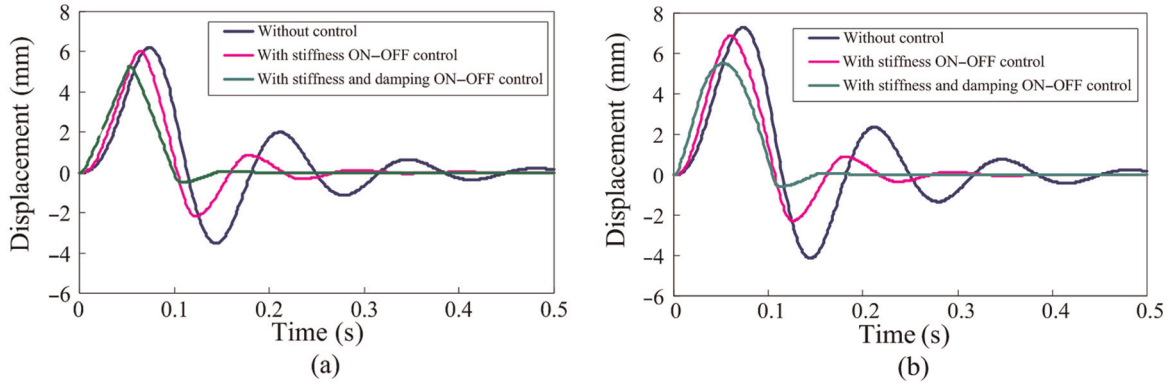

Figure 12. Displacement response to pulse excitation: (a) triangular pulse and (b) half-sinusoid pulse.

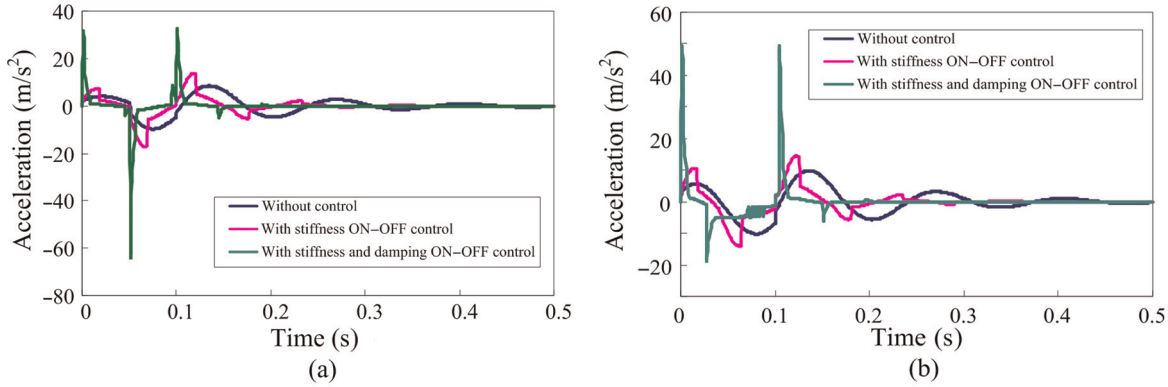

Figure 13. Acceleration response to pulse excitation: (a) triangular pulse and (b) half-sinusoid pulse.

Table 2. Maximum values of the displacement response to pulse excitations.

	Without control (mm)	S ON–OFF control (mm)	S + D ON–OFF control (mm)
Half-sinusoid pulse	7.29	6.88	5.51
Triangular pulse	6.20	6.04	5.28

S ON–OFF: stiffness ON–OFF control; S + D ON–OFF: stiffness + damping force ON–OFF control.

Response to Pulse Base Excitations

To further evaluate the as-designed vibration isolation system, the responses of the payload to pulse base excitations were simulated with the same parameters used in the previous experiments. In the simulation (Figures 12 and 13), two pulse base excitations were used to excite the vibration system. Figure 12(a) is the response to a triangular pulse excitation, and Figure 12(b) is the response to a half-sinusoid pulse excitation. Both the pulse base excitations lasted for 0.1 s. From the figure, it can be seen that under the ON–OFF control, the maximum values of the responses decrease, and the time for eliminating the disturbance caused by the pulse excitation is shortened. Table 2 tabulates the maximum values of the displacement response of the payload to pulse excitations. Figure 13 shows the acceleration response of the payload to the pulse excitation. It can be seen that under ON–OFF control, the acceleration response decreases except for some leaps, which may be due to the sudden change of the stiffness and damping. Overall, the proposed MRE-based vibration isolator shows a good performance under ON–OFF control.

Conclusion

A novel MRE-based tunable stiffness and damping vibration isolator was proposed. The stiffness is controlled by the current applied to the magnetic excitation coil, and the damping is controlled by the feedback gain of the voice coil motor. Therefore, this system is very simple and easy to be used in practical system. Both the experimental results and simulation results indicate that the proposed MRE-based vibration isolator has a good performance using stiffness and damping ON–OFF control. The vibration of the payload to sinusoid excitation, random excitation, and pulse excitation can be suppressed significantly.

Funding

The authors gratefully acknowledge the financial support from NSFC (Grant No. 11072234), SRFDP of China (Project No. 20093402110010), and the Fundamental Research Funds for the Central Universities (No. WK2090000002).

References

Carlson JD and Jolly MR (2000) MR fluid, foam and elastomer devices. *Mechatronics* 10(4–5): 555–569.

Chen L, Gong XL and Li WH (2008) Damping of magnetorheological elastomers. *Chinese Journal of Chemical Physics* 21(6): 581–585.

Deng HX, Gong XL and Wang LH (2006) Development of an adaptive tuned vibration absorber with magnetorheological elastomer. *Smart Materials and Structures* 15(5): N111–N116.

Dyke SJ, Spencer BF, Sain MK and Carlson JD (1998) An experimental study of MR dampers for seismic protection. *Smart Materials and Structures* 7(5): 693–703.

Farshad M and Le Roux M (2005) Compression properties of magnetostrictive polymer composite gels. *Polymer Testing* 24(2): 163–168.

Ginder JM, Nichols ME, Elie LD and Clark SM (2000) Controllable-stiffness components based on magnetorheological elastomers. *Proceedings of SPIE* 3985: 418–425, doi:10.1117/12.388844.

Ginder JM, Nichols ME, Elie LD and Tardiff JL (1999) Magnetorheological elastomers: Properties and applications. *Proceedings of SPIE* 3675: 131–138, doi:10.1117/12.352787.

Ginder JM, Schlotter WF and Nichols ME (2001) Magnetorheological elastomers in tunable vibration absorbers. *Proceedings of SPIE* 4331: 103–110, doi:10.1117/12.432694.

Gong XL, Zhang XZ and Zhang PQ (2005) Fabrication and characterization of isotropic magnetorheological elastomers. *Polymer Testing* 24(5): 669–676.

Hitchcock GH, Gordaninejad F and Fuchs A (2006) Controllable magneto-rheological elastomer vibration isolator, US Patent 7086507.

Jansen LM and Dyke SJ (2000) Semiactive control strategies for MR dampers: Comparative study. *Journal of Engineering Mechanics, ASCE* 126(8): 795–803.

Lerner AA and Cunefare KA (2008) Performance of MRE-based vibration absorbers. *Journal of Intelligent Material Systems and Structures* 19(5): 551–563.

Li WH and Zhang XZ (2010) A study of the magnetorheological effect of bimodal particle based magnetorheological elastomers. *Smart Materials and Structures* 19(3): 035002.

Liu YQ, Matsuhisa H and Utsuno H (2008) Semi-active vibration isolation system with variable stiffness and damping control. *Journal of Sound and Vibration* 313(1–2): 16–28.

Liu YQ, Matsuhisa H, Utsuno H and Park JG (2005) Vibration isolation by a variable stiffness and damping system. *JSME International Journal, Series C: Mechanical Systems, Machine Elements and Manufacturing* 48(2): 305–310.

Nagarajaiah S and Sonmez E (2007) Structures with semiactive variable stiffness single/multiple tuned mass dampers. *Journal of Structural Engineering, ASCE* 133(1): 67–77.

Ni ZC, Gong XL, Li JF and Chen L (2009) Study on a dynamic stiffness-tuning absorber with squeeze-strain enhanced magnetorheological elastomer. *Journal of Intelligent Material Systems and Structures* 20(10): 1195–1202.

Opie S and Yim W (2009) Design and control of a real-time variable stiffness vibration isolator. *2009 IEEE/ASME International Conference on Advanced Intelligent Mechatronics*, Vols. 1–3, 380–385.

Popp KM, Kroger M, Li WH, Zhang XZ and Kosasih PB (2010) MRE properties under shear and squeeze modes and applications. *Journal of Intelligent Material Systems and Structures* 21(15): 1471–1477.

Xu ZB, Gong XL, Liao GJ and Chen XM (2010) An active-damping-compensated magnetorheological elastomer adaptive tuned vibration absorber. *Journal of Intelligent Material Systems and Structures* 21(10): 1039–1047.

Yang JN, Kim JH and Agrawal AK (2000) Resetting semiactive stiffness damper for seismic response control. *Journal of Structural Engineering, ASCE* 126(12): 1427–1433.

Yang JN, Wu JC and Li Z (1996) Control of seismic-excited buildings using active variable stiffness systems. *Engineering Structures* 18(8): 589–596.

Yu M, Dong XM, Choi SB and Liao CR (2009) Human simulated intelligent control of vehicle suspension system with MR dampers. *Journal of Sound and Vibration* 319(3–5): 753–767.

Zhou Q, Nielsen SRK and Qu WL (2008) Semi-active control of shallow cables with magnetorheological dampers under harmonic axial support motion. *Journal of Sound and Vibration* 311(3–5): 683–706.